online data

Differential expression of a C-terminal splice variant of phosphatidylinositol transfer protein β lacking the constitutive-phosphorylated Ser^{262} that localizes to the Golgi compartment

Clive P. MORGAN*, Victoria ALLEN-BAUME*, Marko RADULOVIC†, Michelle LI*, Alison SKIPPEN* and Shamshad COCKCROFT*[1]

*Lipid Signalling Group, Department of Physiology, University College London, 21 University Street, Rockefeller Building, London WC1E 6JJ, U.K., and †Department of Medicine, University College London, WC1E 6JJ, U.K.

Mammalian PITPβ (phosphatidylinositol transfer protein β) is a 272-amino-acid polypeptide capable of transferring PtdIns, PtdCho and SM (sphingomyelin) between membrane bilayers. It has been reported that Ser^{262} present in the C-terminus of PITPβ is constitutively phosphorylated and determines Golgi localization. We provide evidence for the expression of an sp (splice) variant of PITPβ (PITPβ-sp2) where the C-terminal 15 amino acids of PITPβ-sp1 are replaced by an alternative C-terminus of 16 amino acids. PITPβ-sp1 is the product of the first 11 exons, whereas PITPβ-sp2 is a product of the first 10 exons followed by the twelfth exon – exon 11 being 'skipped'. Both splice variants are capable of PtdIns and PtdCho transfer, with PITPβ-sp2 being unable to transport SM. PITPβ is ubiquitously expressed, with the highest amounts of PITPβ found in HL60 cells and in rat liver; HL60 cells express only PITPβ-sp1, whereas rat liver expresses both sp variants in similar amounts. In both cell types, PITPβ-sp1 is constitutively phosphorylated and both the PtdIns and PtdCho forms of PITPβ-sp1 are present. In contrast, PITPβ-sp2 lacks the constitutively phosphorylated Ser^{262} (replaced with glutamine). Nonetheless, both PITPβ variants localize to the Golgi and, moreover, dephosphorylation of Ser^{262} of PITPβ-sp1 does not affect its Golgi localization. The presence of PITPβ sp variants adds an extra level of proteome complexity and, in rat liver, the single gene for PITPβ gives rise to seven distinct protein species that can be resolved on the basis of their charge differences.

Key words: Golgi, lipid transfer proteins, phosphatidylinositol (PtdIns), phosphorylation, phosphatidylinositol transfer protein (PITPβ), splice variants.

INTRODUCTION

Mammalian PITPα and PITPβ (phosphatidylinositol transfer proteins α and β) are 35 kDa soluble lipid transfer proteins which can bind a single molecule of PtdIns or PtdCho. This binding property facilitates lipid solubilization and exchange between different membrane compartments in cell-free systems [1,2] and suggests the involvement of PITPs in inter-organelle lipid transport reactions *in vivo*. *In vivo*, PITPα and PITPβ appear to have distinct roles: a decrease in PITPα protein by 80 % contributes to the neurodegenerative phenotype of the mouse *vibrator* mutation [3], and mice completely devoid of PITPα exhibit spinocerebellar degeneration, intestinal and hepatic steatosis and hypoglycaemia [4]. In contrast, ablation of the PITPβ gene is embryonically lethal [5]. Human PITPα and PITPβ share 77 % sequence identity and 94 % sequence similarity and the most obvious difference resides in the C-terminal 20 amino acids (Figure 1A; residues highlighted in bold type). In addition, orthologues of PITPα and PITPβ in other mammals, including rat, mouse, cow and dog, share a very high primary sequence conservation (between 95 and 99 %). For example, human PITPα differs from rat PITPα by two conservative substitutions and by one amino acid deletion, whereas PITPβ differs by six conservative substitutions. Moreover, the structures of rat PITPα and PITPβ loaded with PtdCho and human PITPα loaded with PtdIns reveal minimal differences in protein conformation [6–8]. Nonetheless, PITPα and PITPβ differ in their cellular localization: PITPα is primarily found in the cytosol and nucleus, whereas PITPβ is found associated with the Golgi complex [9,10]. It has been reported that the Golgi localization of PITPβ is dependent on the C-terminal constitutively phosphorylated residue Ser^{262}, which is absent in PITPα [11,12]. In the present study we report on the characterization and expression of an sp (splice) variant of PITPβ which differs at the C-terminus. The sp variant PITPβ-sp2 (the original PITPβ is referred to here as PITPβ-sp1 and the newly characterized variant as PITPβ-sp2) shows diminished PtdCho and PtdIns lipid transfer activities *in vitro* and is also Golgi-localized, despite the absence of the critical Ser^{262} residue. Of the different rat tissues examined, PITPβ was most highly expressed in liver, with both sp variants being expressed at similar levels. Of the cultured cell lines examined, HL60 cells express the highest levels of PITPβ, which was predominantly accounted for by the PITPβ-sp1 isoform. Endogenous PITPβ-sp1 and PITPβ-sp2 were found to bind and transfer both PtdIns and PtdCho, and, additionally, PITPβ-sp1 was constitutively phosphorylated in cells. These different species were readily resolved on IEF (isoelectric-focusing) gels. We conclude that, in the case of PITPβ, a single gene gives rise to at least seven distinct protein species, adding to the proteomic complexity of different cell types. The most striking difference between the two sp variants is the inability of PITPβ-sp2 to transport SM (sphingomyelin) compared with PITPβ-sp1. The differential expression in proliferating cultured cells compared with rat liver tissue suggests that the sp variants have subtle differences in their biological functions and could relate to membrane traffic

Abbreviations used: Ab, antibody; ARF1, ADP-ribosylation factor 1; DMEM, Dulbecco's modified Eagle's medium; FCS, fetal-calf serum; GAPDH, glyceraldehyde 3-phosphate dehydrogenase; GFP, green fluorescent protein; IEF, isoelectric focusing; Ni-NTA, Ni^{2+}-nitrilotriacetate; PITP, phosphatidylinositol transfer protein; PKC, protein kinase C; λ-PPase, lambda protein phosphatase; RT-PCR, reverse-transcription PCR; SM, sphingomyelin; sp, splice; WGA, wheat-germ agglutinin.

[1] To whom correspondence should be addressed (email s.cockcroft@ucl.ac.uk).

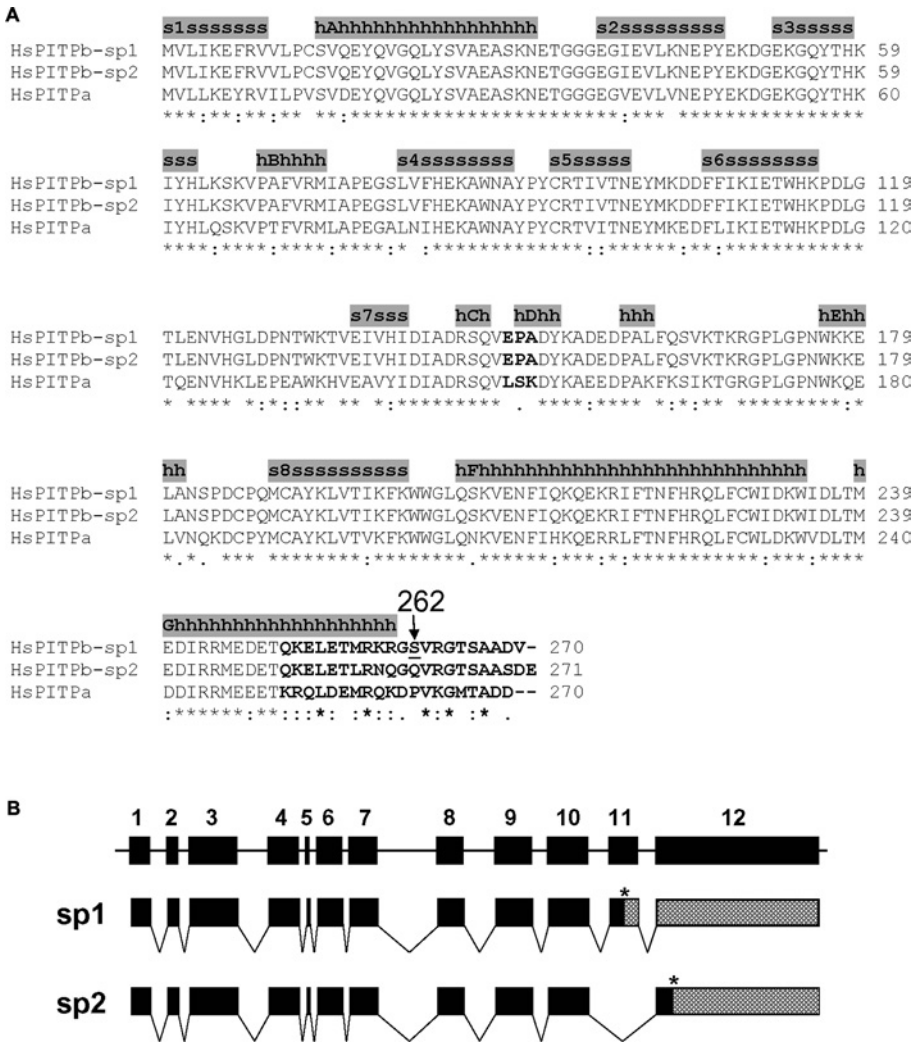

Figure 1 PITP isoform sequence analysis

(**A**) Sequence alignment of human PITPα (HsPITPa) and the two sp variants of human PITPβ (HsPITPb-sp1 and -sp2). The secondary structure of human PITPα is indicated above the sequence. The seven α-helices (h) and the eight β-sheets (s) are labelled A–G and 1–8 respectively. Swiss-Prot Accession numbers are: PITPα, Q00169; PITPβ-sp1, P48739-1; and PITPβ-sp2, P48739-2. (**B**) Schematic diagram showing how the sp variants of PITPβ are derived. Exons are shown as black boxes and introns as lines (not to scale). The stop codon in each transcript is shown with an asterisk (*). These transcripts can be found on chromosome 22 at location 26,572,214–26,639,772. Pre-mRNA splicing of the transcripts of gene ENSG00000180957 leads to the formation of two protein products. Transcript 1 (ENST00000335272) leads to the generation of peptide ENSP00000334738 (sp1). Transcript 2 (ENST00000320996) leads to the generation of peptide ENSP00000321266 (sp2) (Ensembl reference numbers).

during cell division, as opposed to membrane traffic in the secretory pathway.

EXPERIMENTAL

Culture of HL60 and COS-7 cells

HL60 cells and COS-7 cells were cultured as previously described [13].

Immunological reagents

Abs (antibodies) to PITPβ-sp1 were a mouse monoclonal Ab, designated Ab:1C1, raised against whole protein and a rabbit polyclonal Ab raised against a C-terminal peptide (CRKRGSVRGTSAADV), designated Ab:673. The mouse monoclonal Ab was purified using Protein G and the polyclonal Ab was sequentially purified from serum using the peptide immunogen coupled to NHS (*N*-hydroxysuccinimido)-Sepharose (Amersham) followed by phosphorylated peptide, RKRGpS^{262}VRGTSAADV (where pS is phosphoserine), resulting in an Ab specific for non-phosphorylated PITPβ-sp1. Other Abs used were: an affinity-purified rabbit polyclonal PITPα Ab (Ab:674) [13], an affinity-purified rabbit polyclonal anti-ARF1 [anti-(ADP-ribosylation factor 1)] Ab (Ab:679) [14], a mouse-monoclonal Ab (H1029) to the His_6 (hexahistidine) tag (Sigma), an anti-EGFP [anti-(enhanced green fluorescent protein)] Ab (BD Biosciences) and a polyclonal Ab to GM130 (a gift from Dr Martin Lowe, School of Biological Sciences, University of Manchester, Manchester, U.K.).

Identification of sp variants by RT-PCR (reverse-transcription PCR)

HL60 cells were differentiated with 1.25 % (v/v) DMSO, and human neutrophils were prepared from buffy-coat residues. Cells were homogenized by vortex-mixing in guanidinium thiocyanate solution (RLT buffer; Qiagen, Crawley, Sussex, U.K.)

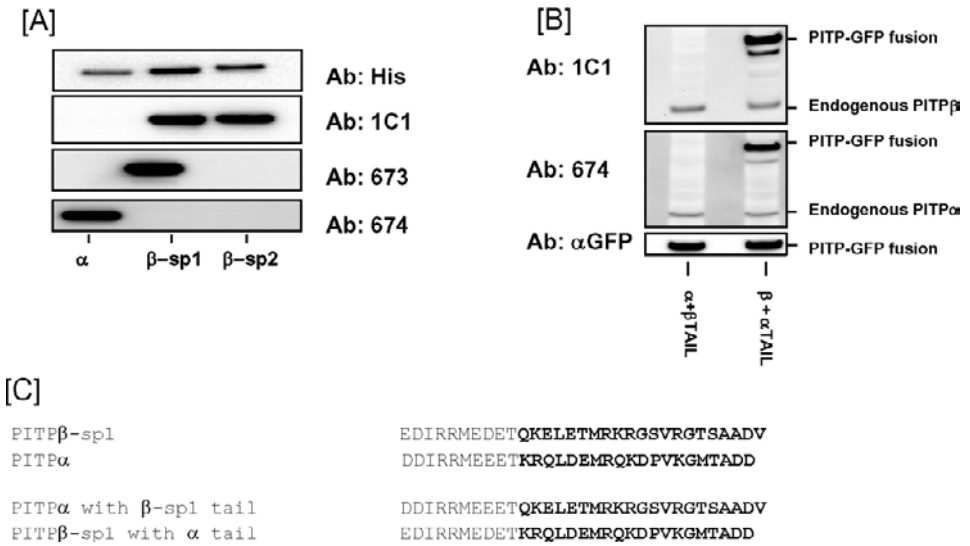

Figure 2 Specificity of PITP Abs

(**A**) His-tagged recombinant proteins PITPα, PITPβ-sp1 and PITPβ-sp2 were probed with four Abs, namely Ab:1C1 made against PITPβ-sp1, Ab:673 made against the C-terminus of PITPβ-sp1, Ab:674 made against the C-terminus of PITPα and a monoclonal Ab to the His_6 fusion tag (Sigma). (**B**) COS-7 cells were transfected with GFP–PITP chimaeras using Lipofectamine® Plus. Western blots of lysates (25 μg) were probed with Ab:1C1, Ab:674 and Ab:anti-GFP. (**C**) Chimaeras used for the analysis in (**B**).

supplemented with 0.1 M 2-mercaptoethanol. Total RNA was then isolated with the RNeasy mini kit (Qiagen). A 1 μg portion of total RNA was reverse-transcribed with MMLV (Moloney-murine-leukaemia virus) reverse transcriptase (Promega, Southampton, U.K.) using dT primers. cDNA synthesized from total RNA isolated from various rat organs was purchased from Clontech (Oxford, U.K.). A cDNA equivalent corresponding to 50 ng (HL60 cells) or 15 ng (human neutrophils) of total RNA was amplified in each reaction. The primers used for PCR were 5′-TCC CCA GAT GTG TGC CTA TAA G -3′ (human PITP, sense); 5′- CGC TTG TTC CCC TCA CTT GAC -3′ (human PITP, antisense); 5′- GCT GGT GAC CAT CAA GTT CAA G-3′ (rat PITP, sense); 5′-TGG AAA CAT CCG TCA ACA CTG -3′ (rat PITP, antisense); 5′-GTC ACC AGG GCT GCT TTT AAC -3′ [human GAPDH (glyceraldehyde 3-phosphate dehydrogenase), sense]; 5′- TGC TTC ACC ACC TTC TTG ATG -3′ (human GAPDH, antisense) and 5′-TCA ACG ACC CCT TCA TTG AC -3′ (rat GAPDH, sense); 5′-TGC TTC ACC ACC TTC TTG ATG -3′ (rat GAPDH, antisense). As a control of mRNA input, GAPDH mRNA levels were determined for each sample in separate RT-PCR reactions. The PCR reactions contained dNTPs and buffer as supplied by the manufacturer, 500 pM of each specific primer and 2.5 units *Taq* polymerase (Qiagen). Transcripts were amplified for 36 cycles with rat PITP primers (30 s at 94 °C, 30 s at 58 °C, 30 s at 72 °C) and 25 cycles for rat GAPDH primers (30 s at 94 °C, 30 s at 58 °C, 45 s at 72 °C), followed by 7 min at 72 °C. Human PITP was amplified for 30 cycles from HL60 cells and 34 cycles from human neutrophils. Human GAPDH was amplified for 19 cycles from HL60 cells and 23 cycles from human neutrophils. The PCR products were analysed by 2%-(w/v)-agarose-gel electrophoresis, stained with ethidium bromide and visualized by UV illumination. For GAPDH amplification, PCR was performed with different cycle numbers to ensure that the amplification was occurring in the linear range. One representative of each rat and human PITP-amplified PCR fragment was sequenced and found to be identical with published sequences (GenBank® accession numbers: human PITPβ-sp2, BC031427; human PITPβ-sp1, BC018714; rat PITPβ-sp2, BC061538 and rat PITPβ-sp1, D21132).

Quantification of PITPβ in rat tissue and cell lines

Lysates from cell lines and rat tissues were prepared in RIPA buffer (50 mM Tris, pH 7.5, 150 mM NaCl, 1 % Nonidet P40, 0.5 % deoxycholate and 0.1 % SDS) with the addition of mammalian cell protease inhibitors (Sigma). Lysates were centrifuged at 15000 ***g*** for 30 min at 4 °C to remove cell debris and PITPβ was quantified by Western blot using recombinant PITPβ-sp1 as a standard [15]. PITPβ was detected with Ab:1C1, which detects both sp variants (see Figure 2).

Analysis of HL60 PITPβ by IEF

Portions (100 ml each) of HL60 cells (10^6/ml; 80 % confluent) were incubated with no additions (control), 1 ml of DMSO (DMSO control) or 1 ml of GF 109205X (bisindolemaleimide I) (1 mM dissolved in DMSO; final concn. 10 μM) overnight. After 16 h, the cells were pelleted at 2500 ***g***, washed once with PBS and resuspended in 1 ml of PBS. The total numbers of cells were counted and results were as follows: control cells, 1.55×10^8; DMSO control, 1.64×10^8; inhibitor, 1.61×10^8. The cells were transferred to an Eppendorf tube, pelleted at 2500 ***g***, and the supernatant removed. The cell pellet was then frozen in liquid nitrogen and stored at −80 °C. Lysates were prepared by sonication (three 3 s pulses) on salted ice/water (approx 0 °C) in 300 μl of PBS containing 20 μl each of protease and phosphatase (I and II) inhibitor cocktails (Sigma). Lysates were then centrifuged at 100000 ***g***, and the supernatant (cytosol) was removed. The cytosol was desalted to 1 ml of water and concentrated to 600 μl using a YM-10 Centricon membrane (Millipore) and the protein content analysed. The protein contents were as follows: control, 16.6 mg/ml; DMSO control, 12.8 mg/ml; and the sample treated with inhibitor, 16.6 mg/ml. For lipid exchange, a sample of desalted cytosol (83–89 μg) was incubated with brain PtdIns or egg-yolk PtdCho vesicles (5 μg of lipid) for 10 min at 30 °C in a

total volume of 20 μl. The samples were directly loaded on to a pH 4–7 Immobiline IEF gel (Amersham) as described previously [13].

Preparation of rat liver cytosol enriched in PITPβ

Rat liver was homogenized in 50 mM Tris, pH 7.6, supplemented with protease and phosphatase inhibitor cocktails (Sigma). The homogenate was centrifuged to pellet membranes and insoluble material at 100 000 ***g*** at 4 °C. The supernatant was filtered through a 0.450-μm-pore-size membrane, and concentrated using an Amicon pressure-filtration device with a 10 kDa-cut-off membrane, resulting in a protein concentration of 92 mg/ml. PITPβ from 460 mg of the supernatant was resolved by gel filtration using a Hi-Load Superdex-75 HR 26/60 (Amersham) column. PITPβ-containing fractions were located by Western blotting with PITPβ-specific Abs (Ab:1C1). Fractions containing PITPβ were pooled and proteins were analysed by SDS/PAGE and IEF [13].

Samples were also pretreated with λ-PPase (lambda protein phosphatase; New England Biolabs) for 30 min at 30 °C. A 180 μg portion of the combined liver fractions was incubated with 2000 units of λ-PPase in 1 × λ-PPase Reaction Buffer (New England Biolabs), supplemented with 2 mM $MnCl_2$ in a total volume of 100 μl. At the end of the incubation, 10 μl of water or 10 μl of PtdIns (1 mg/ml in water) was added for a further 5 min at 30 °C. A 30 μg portion was analysed by Western Blotting and probed with both Ab:1C1 and Ab:673.

Analysis of PITPβ sp variants for lipid transfer and lipid binding

The Mammalian Gene Collection (MGC) Clone (4341137) for PITPβ-sp2 was obtained from MRC gene service. The PITPβ DNA insert was amplified by PCR using appropriate primers and inserted into a mammalian expression vector (pEGFP-C1; Clontech) and a bacterial expression vector (pRSETB; Invitrogen). Protein was expressed in *Escherichia coli* and purified using Ni-NTA (Ni^{2+}-nitrilotriacetate) resin (Qiagen) as previously described [16]. The proteins were additionally purified by size-exclusion chromatography using a Hi-Load Superdex-75 26/60 (Amersham) column. Peak fractions were pooled, concentrated, and the total protein determined. Proteins were analysed by SDS/PAGE and PITPβ content was monitored (using AIDA software) to ensure that equal quantities of protein could then be assayed for lipid transfer as described [15] with the following modifications. Lipid transfer was assayed in permeabilized HL60 cells labelled with [^{3}H]inositol or with [^{3}H]choline as a donor compartment to monitor transfer of PtdIns and choline-labelled lipids (PtdCho and SM) to liposomes as an acceptor compartment exactly as described in [15]. Following transfer to the acceptor compartment, the [^{3}H]choline-labelled lipids were separated by TLC to separate SM from PtdCho. To measure PtdCho and SM transfer separately, lipid transfer was monitored using rat liver mitochondria as acceptor compartment (2 mg/ml protein) and liposomes (500 nmol/ml) in an assay volume of 200 μl at 37 °C for 30 min. For PtdCho transfer, the liposomes contained PtdCho and phosphatidic acid (98:2, w/w) and for SM transfer, the liposomes contained PtdCho, SM and phosphatidic acid (96:2:2, by weight). The modification in the liposome constituents gave improved transfer activity for both PtdCho and SM in comparison with that reported previously [15].

Lipid binding to the PITPs was performed exactly as described in [15]. In brief, His-tagged proteins were incubated with permeabilized HL60 cells prelabelled with [^{14}C]acetate. The PITP proteins were captured using a Ni^{2+} column and the lipids associated with the proteins were analysed by TLC. The amount of radiolabel associated with PITP was expressed as ratio of the amount of protein captured. Quantification of both radioactivity and protein content was done using the the AIDA software.

Transfection of COS 7 cells with PITPβ variants

COS-7 cells were transfected with Lipofectamine® Plus (Invitrogen) using 0.08 μg of DNA/well (or 2 μg/well for Western blotting analysis) as previously described [13].

Treatment of COS-7 cells with GF109203X and with Nocodazole

To disrupt the structure of the Golgi, COS-7 cells were washed twice with Hepes buffer (20 mM Hepes, 137 mM NaCl, 3 mM KCl, 1 mM $CaCl_2$, 2 mM $MgCl_2$, 1 mg/ml glucose and 1 mg/ml BSA) and treated with 20 μM nocodazole or DMSO (vehicle control) in Hepes buffer for 1 h at 37 °C. The dephosphorylation of PITPβ-sp1 was achieved by incubation of COS-7 cells for 16 h with 5 μM GF 109203X in normal growth medium [12]. Following these treatments, cells were fixed with paraformaldehyde and processed for immunofluorescence.

Immunofluorescence

COS-7 cells were cultured on glass coverslips and incubated with primary Abs as indicated, followed by fluorescent (Alexa fluor 488 or 546) conjugated secondary Abs (Molecular Probes) [13].

RESULTS AND DISCUSSION

Sequence analysis

We conducted BLAST searches against the non-redundant NCBI database to identify sequences of PITPs from other species in order to find key determinants that could allow us to identify orthologues of PITPα and PITPβ [17]. Using human PITPβ as a query sequence we identified a total of 90 PITP-related-sequences after removing partial and identical sequences. Because *in silico* gene structure prediction methods often do not correctly annotate the intron–exon structure of genes, some sequences were excluded as the prediction appeared out of line with biological data of known protein sequences. Sequence alignment of 79 PITP-related sequences allowed us to group the PITPs into families, and orthologues of human PITPβ and PITPα were identified in mouse, rat, dog and chimpanzee. In some species, for example the fruitfly *Drosphila melanogaster* and the sea squirt *Ciona intestinalis*, a single PITP [related to PITPNA (≡PITPα) and PITPNB (≡PITPβ) (HUGO Gene Nomenclature Committee Symbol ID)] is found. PITPs in unicellular organisms, such as the protozoan parasite *Encephalitozoon cuniculi* and the cellular slime mould *Dictyostelium discoideum*, were too divergent to be identified as orthologues of either PITP. Many of the sequences were already predicted by automated computational analysis as PITPβ or PITPα (http://www.ncbi.nlm.nih.gov/). A total of 22 sequences could be identified as PITPβ orthologues and seven sequences as PITPα orthologues, on the basis mainly of the identity of their C-terminal residues (see Supplementary Fig. 1S at http://www.BiochemJ.org/bj/398/bj3980411add.htm). PITPα from different species share 95–99 % sequence identity. The sequences identified were supported in most cases by either mRNA, expressed sequence tags or protein [18]. We identified multiple PITPβ sequences in the human, dog, rat and mouse genomes that had the same chromosomal location (chromosome 22 in humans), and were annotated as sp variants that differed at the C-terminus. Figure 1(A) compares the sequence of the human sp variants of PITPβ (sp1 and sp2). For clarity we refer to the original isoform as PITPβ-sp1 and the more recently identified isoform as PITPβ-sp2. The differences between the sp variants of

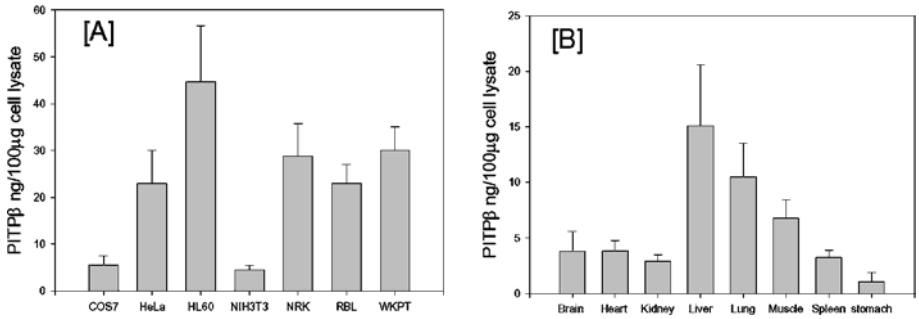

Figure 3 Quantification of total PITPβ in cell lines and rat tissues

Lysates prepared from (**A**) cell lines and (**B**) rat tissues were separated by SDS/PAGE, followed by Western-blot analysis using PITPβ pan Ab (Ab:1C1). On each gel, a concentration range of recombinant PITPβ-sp1 proteins was included and the amount of PITP proteins present in the sample was calculated on the basis of the standards. The results in (**A**) and (**B**) are average values from three independent analyses.

PITPβ also reside at the C-terminus. Of note is the absence of the critical Ser^{262} residue, which is the site of phosphorylation by PKC (protein kinase C) in PITPβ-sp1 [12]. In the sp variant PITPβ-sp2, this residue is glutamine (Q). In Supplementary Figure S1 (http://www.BiochemJ.org/bj/398/bj3980411add.htm), sequences that contain Ser^{262} or Gln^{262} are grouped together (Group 2 and 3 respectively). In the fourth group are sequences where the Ser^{262} is replaced with alanine, glutamic acid or cysteine. The canonical sequence for PKC phosphorylation is $^{S}/_{T}X^{R}/_{K}$ and the motif $^{R}/_{K}$ is found in all of the sequences (highlighted in grey).

The human *PITPNB* gene maps to chromosome 22q12 and analysis of the genomic structure show the presence of 12 exons (Figure 1B). The chromosome band at this location is in synteny with rat, chimp, mouse, chicken and dog [Ensembl v35 (November 2005)]. Details of the genomic organization of the human PITPβ gene and the origin of two transcripts are shown in Figure 1B. Pre-mRNA splicing of the transcripts of GENE: ENSG00000180957 leads to the formation of two protein products, PITPβ-sp1 and PITPβ-sp2. PITPβ-sp1 is a product of the first 11 exons, whereas PITPβ-sp2 is a product of the first 10 exons followed by the twelfth exon, exon 11 being 'skipped'. This accounts for the difference in the C-terminus of the two PITPβ variants formed from a single gene (Figure 1A).

Quantification of total PITPβ

To identify the expression of the PITPβ proteins, we used a monoclonal Ab raised against the whole PITPβ-sp1 protein (Ab:1C1) and a polyclonal peptide Ab raised against the C-terminus of PITPβ-sp1 (Ab:673). Ab specificity was examined using recombinant His-tagged PITP proteins. Anti-polyhistidine was used as a control (Figure 2A). Ab:1C1 recognizes both sp variants of PITPβ, but does not recognize PITPα, whereas Ab:673 only recognizes PITPβ-sp1. Ab:674, made against the C-terminus of PITPα [13], is specific for PITPα, with no cross-reactivity to the PITPβ proteins (Figure 2A).

Since the major difference in sequence between PITPα and the two isoforms of PITPβ is localized at the C-terminus of the protein, we were initially surprised that Ab:1C1 did not recognise PITPα, but recognized both PITPβ isoforms equally well. To confirm that the epitope for Ab:1C1 was not in the C-terminus, we made chimaeras of PITPβ-sp1 with the PITPα tail and of PITPα with β-sp1 tail (Figure 2C). The chimaeras were tagged with GFP (green fluorescent protein) and expressed in COS-7 cells, and lysates were blotted with GFP Abs to show that the fusion proteins were expressed (Figure 2B). Ab:1C1 still recognized PITPβ-sp1 with the PITPα-tail, and, secondly, it did not recognize the PITPα with the PITPβ-sp1 tail. Ab:674 was used to confirm that the chimaeric proteins had acquired the PITPα C-terminus. From this we conclude that Ab:1C1 recognizes an epitope in PITPβ that is distal to the entire C-terminus.

The availability of a pan-PITPβ Ab and a PITPβ-sp1-specific Ab made it possible to infer the quantity of PITPβ-sp2 protein. To identify which cell line or rat tissue would be most appropriate to investigate for protein expression of the sp variants, we quantified the expression levels of PITPβ using the pan-specific Ab:1C1. All cell lines and tissues examined expressed PITPβ without exception, but to various extents (Figures 3A and 3B). In rat tissue, the highest expression of PITPβ protein was found in the liver and, of the cell lines, HL60 cells demonstrated the highest level of PITPβ protein. Most of the cell lines studied (except for COS-7 and NIH 3T3 cells) had elevated PITPβ expression levels when compared with the rat tissues. The difference in expression levels in different tissues probably relates to the function of PITPβ. In the mammary gland, the terminal lobular–alveolar unit is composed of two types of epithelial cells. The inner or luminal epithelial cells, which are potential milk-secretory cells, are surrounded by an outer layer of contractile myo-epithelial cells. Proteomic analysis of normal human luminal and myo-epithelial breast cells identified PITPβ as being expressed at four-times-higher levels in luminal cells compared with myo-epithelial cells [19]. This would suggest that the increased expression might be related to the secretory function of the cell, or, alternatively, to their proliferative status. It should be noted that most breast carcinomas express phenotypic markers that are consistent with an origin from luminal cells.

Analysis of HL60 PITPβ expression and its phosphorylation and lipid binding status

Since HL60 cells express a substantial amount of PITPβ, this cell line was examined for expression of the sp variants. Ab:1C1 recognizes both sp variants of PITPβ, whereas Ab:673 only recognizes PITPβ-sp1 (see Figure 2A) and therefore these two Abs could be used to calculate the expression of the sp forms. Since Ab:673 was purified so that it was specific for non-phosphorylated PITPβ-sp1, we pretreated HL60 cells for 16 h exactly as described with the PKC inhibitor GF109203X (bisindomaleimide I) to dephosphorylate PITPβ-sp1 [12]. A proportion of PITPβ-sp1 was non-phosphorylated in control cells, and this proportion was clearly increased in cytosol from PKC-inhibitor-treated cells (Figure 4A). To examine expression of the sp variant, PITPβ-sp2, we used Ab:1C1 to quantify total PITPβ,

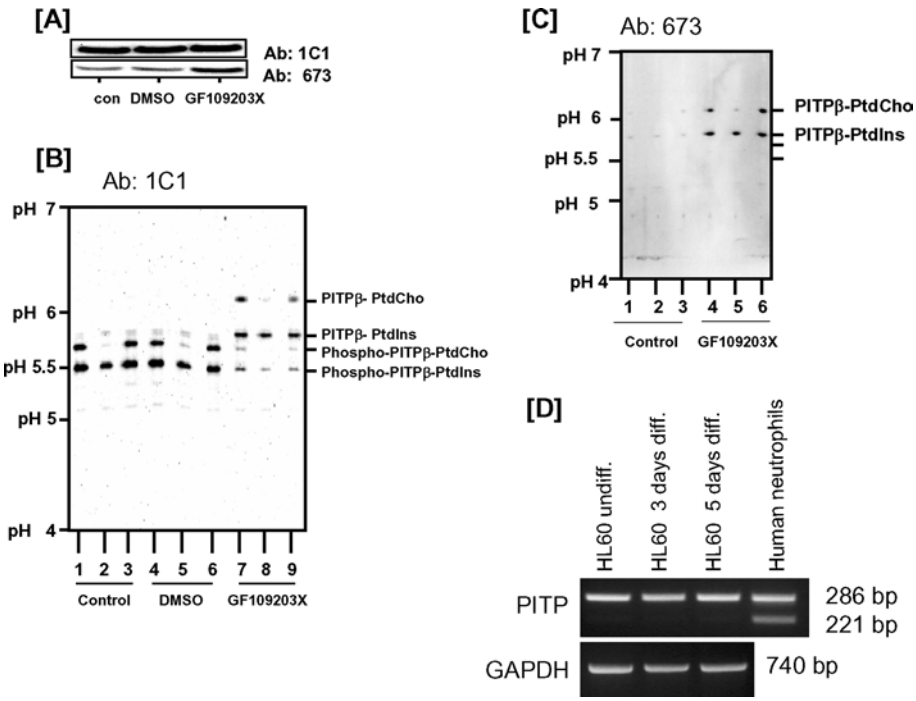

Figure 4 Analysis of the expression of PITPβ sp variants in HL60 cells

(**A**–**C**) HL60 cells were incubated for 16 h with GF 109203 (10 μM) or DMSO vehicle control. Cytosol was prepared and analysed as described below. (**A**) HL60 cytosol (40 μg) from control, DMSO- and GF109203 (10 μM)-treated cells was separated by SDS/PAGE and transferred to PVDF. Membranes were then probed using Ab:1C1 and Ab:673. (**B**, **C**) HL60 cytosol (83–89 μg) from control, DMSO- and GF109203 (10 μM)-treated cells was resolved using native IEF and transferred to PVDF. Membranes were probed with (**B**) Ab:1C1 and with (**C**) Ab:673. Cytosol was incubated with PtdIns (lanes 2, 5 and 8) or PtdCho vesicles (lanes 3, 6 and 9) prior to electrophoresis. pI values for PITPα-PtdCho, PITPα-PtdIns, phospho-PITPα-PtdCho and phospho-PITPα-PtdIns are 6.1, 5.8, 5.7 and 5.5 respectively. (**D**) Human cDNA was generated from control HL60 cells, and HL60 cells differentiated with DMSO for 3 and 5 days. Human neutrophil cDNA was included as a control. Top panel: a 286 bp fragment (PITPβ-sp1) and a 221 bp fragment (PITPβ-sp2) were amplified from cDNA using human-specific PITPβ primers. Bottom panel: a 740 bp fragment was amplified from the cDNA using GAPDH primers. PCR products were electrophoresed on 2 % agarose, stained with ethidium bromide and visualized by UV.

and used Ab:673 to monitor the amount of PITPβ-sp1 in PKC-inhibitor-treated cells using recombinant PITPβ standards (results not shown). From this analysis, approx. 85–90 % of the PITPβ present in HL60 cells could be accounted for by PITPβ-sp1. Since dephosphorylation by the PKC inhibitor is incomplete (see Figure 4B), this would suggest that, in HL60 cells, PITPβ-sp1 is the predominant species.

By analogy with PITPα, it was anticipated that PITPβ-sp1 would be resolved by native IEF into two distinct forms, owing to the net difference in charge between PtdIns and PtdCho [13]. In addition, since IEF would also report on the phosphorylation status of PITPβ-sp1, we also compared the IEF profiles in cytosol prepared from untreated and PKC-inhibited HL60 cells. In control cells (and DMSO-control cells), the two major forms of PITPβ comprised of phosphorylated PITPβ loaded with PtdIns and with PtdCho (Figure 4B, lanes 1 and 4). In cells treated with the PKC inhibitor, four forms were clearly visible – the non-phosphorylated forms of PtdIns- and PtdCho-loaded proteins predominated with residual amounts of the phosphorylated forms (Figure 4B, lane 7). Dephosphorylation is not complete, as some phosphorylated species are still observed. The cytosol from control and treated cells was also incubated with PtdIns or PtdCho vesicles prior to IEF. When incubated with PtdIns, the PtdCho form of PITPβ was readily converted into the PtdIns form (Figure 4B; compare lanes 1 with lanes 2, lanes 4 with lanes 5 and lanes 7 with lanes 8). In contrast, incubation of cytosol with PtdCho vesicles does not readily cause a shift to PtdCho binding (compare lanes 1 with lanes 3, lanes 4 with lanes 6 and lanes 7 with lanes 9). Taken together, four bands are observed on IEF which correspond to the PtdCho-loaded PITPβ-sp1 (pI 6.1), PtdIns-loaded PITPβ-sp1 (pI 5.8) and their Ser^{262}-phosphorylated forms (PtdCho-loaded, pI 5.7 and PtdIns-loaded, pI 5.5) (Figure 4B).

When parallel samples were analysed by IEF and probed using Ab:673, only a faint signal for PITPβ is detected in control cells and, upon treatment with the inhibitor, Ab:673 detects two bands which correspond to non-phosphorylated PITPβ loaded with PtdIns and PtdCho (Figure 4C). Incubation with lipid vesicles again causes a shift from the PtdCho form to the PtdIns form, but not vice versa. From this analysis, we conclude that the majority of PITPβ-sp1 is phosphorylated, and can be substantially dephosphorylated by treatment with the PKC inhibitor, and that PITPβ-sp1 is loaded with both PtdIns and with PtdCho. No additional bands were observed on IEF that could not be accounted for by the presence of PITPβ-sp1. We conclude that PITPβ-sp2 protein is not found in significant amounts in HL60 cells. As no PITPβ-sp2 protein was detected in HL60 cells, we decided to analyse mRNA levels for the PITPβ isoforms. Using primers designed to amplify cDNA for both sp1 and sp2, we found no evidence of sp2 mRNA in either control or DMSO-differentiated HL60 cells (Figure 4D). Using the same primers we were clearly able to amplify products for both sp variants in human neutrophils, indicating the presence of both forms in cells of primary origin.

Analysis of PITPβ expression in rat liver tissue

From the above analysis, HL60 cells appear to express predominantly PITPβ-sp1. We next analysed PITPβ from rat liver tissue, as it expresses the highest amount of PITPβ (see

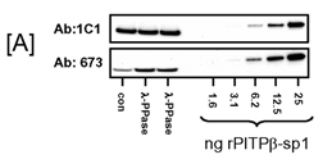

Sample	Ab: 1C1-ng PITPβ	Ab: 673 ng PITPβ–sp1	% PITPβ–sp1 accounted for	% PITPβ unaccounted for
control	20.7	5.2	25.3	74.7
λ-PPase	22.0	9.2	41.5	58.5

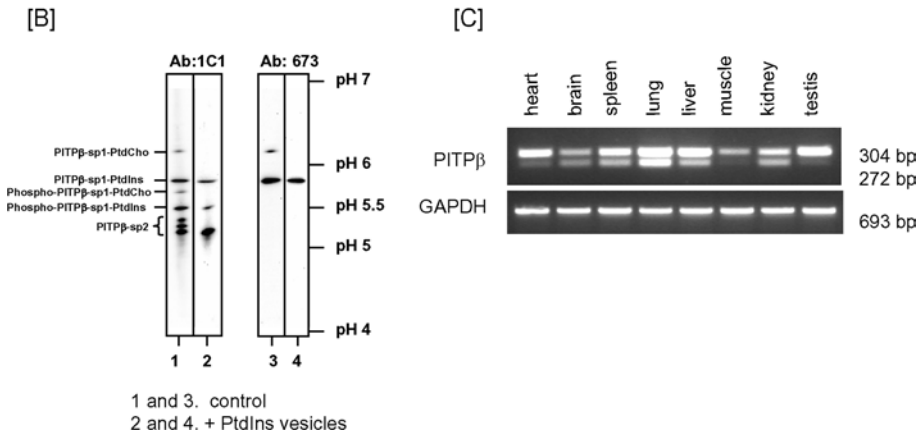

Figure 5 PITPβ-sp1 and -sp2 proteins are present in rat liver tissue

Rat liver cytosol was fractionated by gel filtration, and fractions enriched in PITPβ were combined. (**A**) PITPβ was quantified in the partially purified fractions using recombinant PITPβ-sp1. Samples were additionally pre-treated with λ-PPase to dephosphorylate PITPβ-sp1. A 30 μg portion was analysed by Western blotting and probed with Ab:1C1 and Ab:673. On each gel, a concentration range of recombinant PITPβ-sp1 was included and the amount of PITP proteins calculated on the basis of standards using AIDA software. The results are tabulated, and only 40 % of the total PITPβ is due to PITPβ-sp1, the remainder (60 %) being attributed to PITPβ-sp2. (**B**) Rat liver fractions were analysed by IEF. Samples were desalted to water and 44 μg was resolved using Immobiline 4–7 pre-cast gels swollen in water + 2.5 % Pharmalyte 3–10 at 13.2 kV · h. Where indicated, 2 μg of PtdIns vesicles was incubated with the sample for 5 min at 30 °C prior to IEF. After Western blotting, membranes were probed with Ab:1C1 and Ab:673. (**C**) A panel of rat tissue cDNAs was obtained from Clontech. Upper panel: a 304 bp fragment (PITPβ-sp1) and a 272 bp fragment (PITPβ-sp2) were amplified in from Rat panel 1 using PITPβ primers. Lower panel: a 693 bp fragment was amplified from the cDNA panel using GAPDH primers. PCR products were electrophoresed on 2 % agarose, stained with ethidium bromide, and visualized under UV light.

Figure 3B) and could be obtained in significant amounts. For this analysis, crude rat liver cytosol did not contain sufficient PITPβ for analysis on IEF, and therefore PITPβ was enriched using gel filtration. Dephosphorylation using λPPase led to an increase in Ab staining when Ab:673 was used (Figure 5A), demonstrating that rat liver PITPβ-sp1 is also phosphorylated. The Western blots were quantified and, from this analysis, we could conclude that PITPβ-sp1 only accounted for $\sim$40 % of the total PITPβ, assuming complete dephosphorylation by λPPase (Figure 5A).

Rat liver PITPβ was then analysed by native IEF (Figure 5B). Ab:673 revealed two bands, identified as non-phosphorylated PITPβ-sp1 loaded with PtdCho and with PtdIns (Figure 5B, lane 3). The PtdCho form was readily converted into the PtdIns form when incubated with PtdIns vesicles (Figure 5B, lane 4). Ab:1C1 identified seven bands in total, four of which were accounted for by PITPβ-sp1 (Figure 5B, lane 1). [The identity of the phosphorylated species was confirmed by incubating the sample with λ-phosphatase (results not shown).] The three new bands most likely represent the sp variant PITPβ-sp2. When incubated with PtdIns vesicles (Figure 5B, lane 2), the three bands collapsed into a single band, suggesting that they represent the same protein, but loaded with different lipids or with no lipid. We conclude that rat liver expresses both sp variants of PITPβ and, judging by the intensity of the bands, both proteins are present at similar levels. This conclusion is supported by the quantitative analysis (Figure 5A).

The protein expression data are also supported by the presence of mRNA for both sp variants in rat liver (Figure 5C). PCR analysis of cDNA obtained from different rat tissues (Rat multiple tissue cDNA panel 1; Clontech) revealed bands of expected size corresponding to the expression of both sp variants (Figure 5C). GAPDH was used to standardize the amount of cDNA. PITPβ-sp1 mRNA levels were highest in lung, liver, and testes, followed by heart, spleen and kidney. Lowest levels were found in brain and skeletal muscle. PITPβ-sp2 mRNA levels were high in lung, but were also found in liver. mRNA for PITPβ-sp2 was also observed in spleen, brain, heart and kidney, with skeletal muscle and testes having the lowest levels.

Comparison of the transfer activity and lipid binding properties of recombinant PITPβ-sp1 with PITPβ-sp2

When resolved by IEF, PITPβ-sp2 was found in three bands, which collapsed into a single band when incubated with PtdIns vesicles. This eliminates protein phosphorylation as the cause of differences in IEF and leaves us with the possibility that it may be due to differences in the nature of the bound lipid, lack of lipid or due to protein conformation [20]. It had been previously reported that chicken liver and bovine brain express a PITPβ isoform that could transfer SM; the PITPβ used in those studies was purified from either chicken liver or bovine brain and a fluorescent SM was used for lipid transfer [21,22]. When recombinant PITPβ-sp1 expressed in *E. coli* was examined for SM binding using permeabilized HL60 cells as a source of lipids, the protein bound mainly PtdIns and PtdCho and negligible amounts of SM [15]. Furthermore, the protein showed very little SM transfer activity when permeabilized HL60 cells were used as a donor compartment in the transfer assay [15]. Yet the PITPβ isoform purified from chicken was able to transfer bovine SM from unilamellar vesicles to bovine heart mitochondria [21]. This discrepancy could be explained if it is the PITPβ-sp2 isoform that is able to transfer SM. Our studies with rat liver clearly show

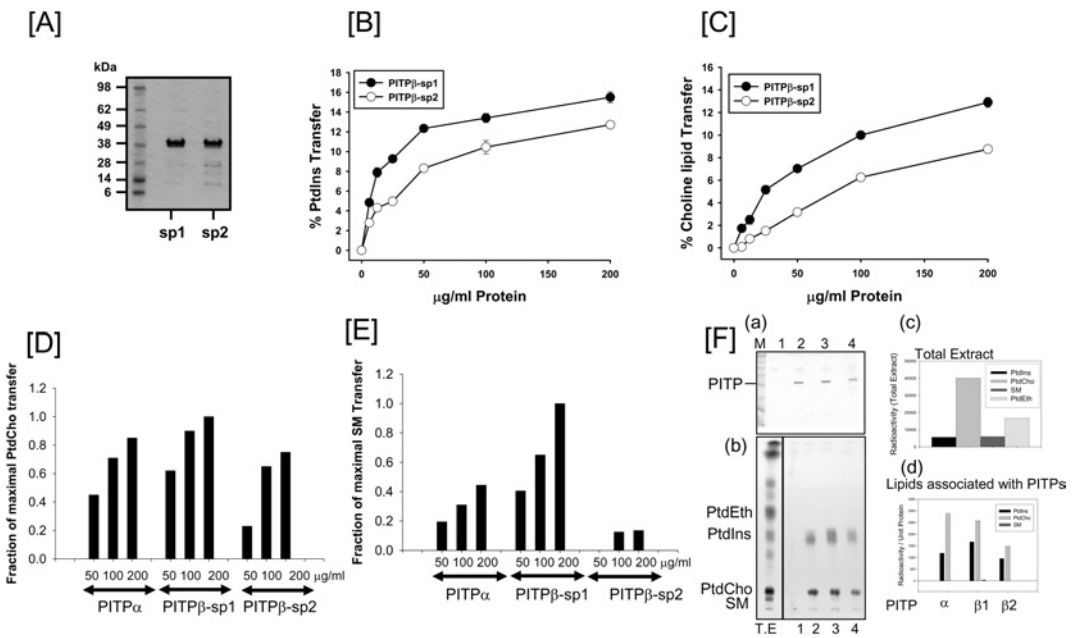

Figure 6 Lipid transfer activity and lipid binding properties of recombinant PITPβ-sp1 and PITPβ-sp2

(**A**) His-tagged recombinant proteins were purified using Ni-NTA, followed by gel-filtration. Protein concentrations were determined, and SDS/PAGE analysis was performed to standardize the proteins. A sample (2 μg) of each standardized protein was analysed by SDS/PAGE and stained with Colloidal Coomassie. (**B**) PtdIns transfer and (**C**) choline lipid transfer were monitored from ^{3}H-labelled (inositol or choline) permeabilized HL60 cells to synthetic liposomes as described. (**D**) PtdCho transfer was monitored using radiolabelled liposomes as donor and mitochondria as acceptor compartments. The liposome composition for PtdCho transfer was PtdCho/phosphatidate (98:2, mol%) and data are expressed as a fraction of maximal transfer. Maximal transfer was ~20%. (**E**) SM transfer was monitored using radiolabelled liposomes as donor and mitochondria as acceptor compartments. Liposome composition for SM transfer was PtdCho/SM:phosphatidate (96:2:2, mol%) and data are expressed as a fraction of maximal transfer. Maximal transfer was ~5%. (**F**) Lipid binding to PITP proteins was monitored after incubation of His-tagged proteins with permeabilized HL60 cells prelabelled to equilibrium with [^{14}C]acetate. The His-tagged proteins were recaptured on the Ni-NTA and recovery was monitored by SDS/PAGE (panel a). The remainder of the sample was extracted and analysed by TLC together with the total extract from the cells (panel b). The levels of radioactivity in the total extract (panel c) and in the lipids associated with the PITPs (panel d) were quantified. T.E, total cell extract. Lane 1, no protein added; lane 2, PITPα; lane 3, PITPβ-sp1; and lane 4, PITPβ-sp2.

that PITPβ-sp2 is present in substantial amounts. We therefore examined the transfer activity of the sp variants of PITPβ for both inositol lipids and for choline-labelled lipids.

We expressed the two PITPβ proteins in *E. coli* and purified them using the histidine tag followed by gel filtration (Figure 6A). Because of impurities in the PITPβ-sp2 preparation, the concentrations of the proteins were calculated using the intensity of the PITPβ-sp1 band. The purified proteins were analysed for both PtdIns and PtdCho/SM transfer as described previously [15]. Lipid transfer was monitored from HL60 cells labelled with [^{3}H]inositol for PtdIns transfer and with [^{3}H]choline for the combined transfer of PC and SM. Both proteins showed transfer activity towards inositol lipids and choline-containing lipids (Figures 6B and 6C), but PITPβ-sp2 was found to be less active for transfer when compared with PITPβ-sp1.

To examine which of the choline lipids were transferred by the PITPβ isoforms, we used an *in vitro* assay which monitors transfer between mitochondria (acceptor compartment) and radiolabelled liposomes as a donor compartment, as described previously [15]. Both PtdCho and SM transfer were monitored alongside for comparison and PITPα was also included. All three PITPs were active in transferring PtdCho (Figure 6D). However, a marked difference was observed for SM transfer (Figure 6E). PITPβ-sp1 shows the highest SM transfer, whereas PITPβ-sp2 shows the least SM transfer activity. Thus, in this *in vitro* assay, SM transfer was highest for PITPβ-sp1, followed by PITPα, then PTPβ-sp2.

From this result it is unlikely that SM binding is responsible for giving rise to the third band on the IEF gel (Figure 5B). We therefore examined which lipid species were bound by the PITPs when added to permeabilized HL60 cells, which had been prelabelled to equilibrium with [^{14}C]acetate. The major lipid species bound to the two sp variants of PITPβ and PITPα were PtdCho and PtdIns (Figure 6F). The relative amounts of the lipids in the total extract is also shown, as is the amount of PtdIns and PtdCho bound to the PITPs expressed as a function of the amount of PITPs recaptured. The amounts of PtdIns and SM in the total cell extract are equivalent, with PtdCho being the dominant lipid. Despite the significant amounts of PtdEtn in the total cell extract, no binding to PtdEtn is evident. The TLC plate was overexposed to reveal any other species of lipid and the only lipid that bound was SM. Although binding to SM was very low (Figure 6F, panel d), it was apparent that the preference is in the order PITPβ-sp1 > PITPα > PITP-sp2 (see Supplementary Figure S2 at http://www.BiochemJ.org/bj/398/bj3980411add.htm), similar to that observed for SM transfer.

From this analysis, we would suggest that PITPβ-sp2 only binds to PtdCho and PtdIns, and the presence of the additional band could be accounted for by the presence of an apo form which is likely to have a different protein conformation [23] compared with the lipid-loaded forms [6–8]. This conclusion is supported by the lesser amounts of lipid associated with the protein and the diminished transfer activity (Figures 6B, 6C and 6F).

Localization of PITPβ sp variants in cells

We expressed the sp variants in COS-7 cells as GFP fusions and examined their localization by confocal microscopy. Expression of the full-length fusion proteins was confirmed by Western blotting with Ab:1C1 and Ab:anti-GFP Abs (Figure 7A) and both sp variants localized at the Golgi (Figure 7B). The cells were co-stained

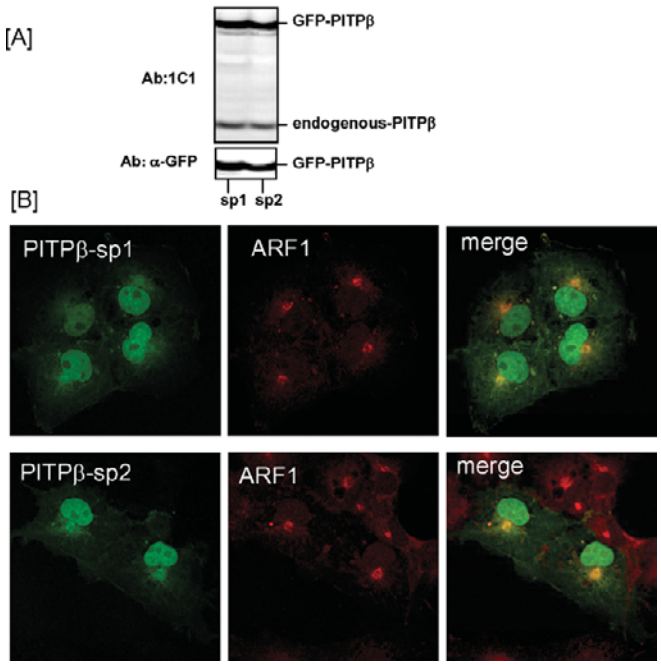

Figure 7 Co-localization of PITPβ isoforms with ARF1

COS-7 cells were transfected with GFP-tagged PITPβ-sp1 or -sp2 using Lipofectamine® Plus. (**A**) Expression of full-length fusion proteins was ascertained by Western blotting. Cell lysates were generated with RIPA buffer, and 15 μg of total protein was used for Ab:1C1, and 30 μg for Ab:anti-GFP. (**B**) Transfected COS-7 cells were also fixed and imaged using confocal microscopy. ARF1 was used as a co-stain to demonstrate Golgi localization of PITPβ isoforms.

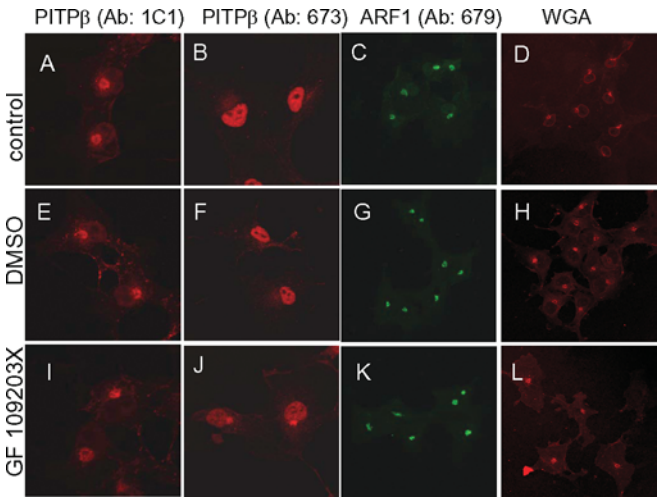

Figure 8 Treatment with PKC inhibitor does not cause loss of PITPβ from the Golgi complex

COS-7 cells were incubated for 16 h with GF 109203 (5 μM) and the cells were fixed and immunostained with PITPβ, AP-1 and ARF Abs to examine Golgi staining and morphology. (**A**–**D**) Control cells; (**E**–**H**) vehicle control (DMSO); (**I**–**L**) GF 109203. The cells were stained with two separate PITPβ Abs, Ab:1C1 (**A**, **E** and **I**), which is a pan-PITPβ Ab, and the polyclonal Ab:673 (**B**, **F** and **J**), which only recognizes the non-phospho form of PITPβ-sp1. An ARF1 Ab (**C**, **G** and **K**) and WGA (**D**, **H** and **L**) was used to stain the Golgi in parallel. Staining of the Golgi with Ab:1C1 is unchanged following treatment with the inhibitor (**A**, **E** and **I**). By contrast, an increased staining of the Golgi is observed when Ab:673 is used on the treated cells (**J**), indicating the accumulation of dephosphorylated protein at the Golgi. The Golgi structure is not affected by the inhibitor, as evidenced by the lack of change in the staining profile of both ARF1 and WGA.

with ARF1, a Golgi marker and the merged images clearly show extensive co-localization. Golgi localization of endogenous PITPβ and both sp variants was further confirmed by treating the cells with nocodazole to disrupt the Golgi (see the Supplementary Figure S3 at http://www.BiochemJ.org/bj/398/bj3980411add.htm).

Since PITPβ-sp2 lacks Ser^{262}, but is still Golgi-localized, this suggested that phosphorylation of Ser^{262} is not the major determinant that dictates Golgi localization of PITPβ-sp1, as reported previously [12]. To examine the importance of phosphorylation of PITPβ-sp1 in determining Golgi localization, we studied the localization of endogenous PITPβ proteins with Ab:1C1 and Ab:673 in control cells and cells treated with GF 109203X to dephosphorylate PITPβ-sp1 (Figure 8). Ab:673 weakly stains the Golgi in the control and DMSO-control cells (Figures 8B and 8F), but readily stains the Golgi in the GF 109203X-treated cells (Figure 8J), confirming that PITPβ-sp1 is mainly phosphorylated in COS-7 cells and that treatment with the PKC inhibitor is effective in causing dephosphorylation. Ab:673 also stains the nuclei, and this is unchanged by the inhibitor, indicating that this staining is likely to be an artifact. ARF1 and WGA (wheat-germ agglutinin) staining confirmed that the Golgi remained intact under these conditions. Collectively, these data demonstrate that Golgi localization is not dependent on the phosphorylation status of PITPβ-sp1.

Conclusions

In the present study we have characterized a Golgi-localized PITPβ sp variant (PITPβ-sp2) that differs at the C-terminus, and evidence for its expression at the mRNA and at the protein level is provided. We show that the choline lipids (PtdCho and SM combined) and PtdIns transfer activity is reduced in PITPβ-sp2 compared with PITPβ-sp1. The most marked difference between the two sp variants is the ability to transfer SM. PITPβ-sp2 is relatively poor at transferring SM compared with PITPβ-sp1. In rat liver, where PITPβ is highly expressed, PITPβ-sp2 represents a substantial proportion of the total PITPβ proteins. In contrast, in HL60 cells, although PITPβ is also highly expressed, the dominant isoform found is PITPβ-sp1. PITPβ-sp1 is mainly phosphorylated in both HL60 cells and in rat liver and pretreatment with either a PKC inhibitor or λ-PPase treatment can effectively dephosphorylate the protein. PITPβ-sp2, on the other hand, lacks Ser^{262}, and thus cannot be phosphorylated. Regardless of the phosphorylation status, both sp variants are Golgi-localized, indicating that the determinant for Golgi localization is either distal to the C-terminus or does not wholly reside in the C-terminus and that another portion of the molecule must be involved. There are only minor differences between PITPα and PITPβ in the remaining body of the sequence, and in Figure 1(A) we highlight the residues [EPA (one-letter code) in PITPβ and LSK in PITPα] which may be a contributory factor towards the localization. In the three-dimensional structure the C-terminus makes close contact with these residues, suggesting that specificity might be dictated by a surface created by the juxtaposition of the C-terminus together with these three residues highlighted in bold type in Figure 1(A).

The identification of two sp isoforms of PITPβ differing solely at the C-terminus is highly relevant, since PITPα is also most divergent from PITPβ at the C-terminus (see Figure 1A). The C-terminus appears to dictate protein–protein interactions; the C-terminus of PITPα specifically binds to DCC (deleted in colon cancer), the receptor for netrin-1 [24]. Netrin-1-stimulated phospholipase C signalling specifically depends on PITPα, although, *in vitro*, phospholipase C signalling is supported by

either PITPα or PITPβ [25]. *In vitro* the PITP proteins function essentially as lipid transfer proteins, albeit with subtle differences in transfer activity. However, judging by the different phenotypes exhibited by mice when the individual genes are deleted would argue for dedicated functions *in vivo*, which is likely to depend on interactions with other proteins [4,5]. In the absence of an Ab to the sp variant, we have only limited information about the expression levels in different cell types. However, it is clear, even from the limited analysis provided here, that they are differentially expressed. The importance of the differential expression of the sp variants may be related to the differences in SM transfer activity, where different cell types make specific use of this capacity for SM transfer. We should stress that SM transfer, although measurable *in vitro*, is unlikely to be of major importance in cells, because SM availability for transfer is highly restricted – the majority of the SM is not accessible to cytosolic PITPs. An alternative possibility is that the sp variants of PITPβ may fulfil specific functions in the cells by their expression levels being regulated in both a time- and a tissue-specific manner, supporting developmental pathways, cell differentiation and proliferation and other processes associated with complex multicellular organisms. We have recently observed that, in dividing cells, PITPβ is re-localized from the Golgi. In metaphase, PITPβ is found along microtubules between the opposing spindle pools; at anaphase and telophase, PITPβ is concentrated on the central spindle; at late telophase it localizes at the mid-zone; and during the late stage of cytokinesis, PITPβ is detected on the interconnecting cytoplasmic bridge (N. Carvou and S. Cockcroft, unpublished work). The Ab that we have used for these studies does not discriminate between the two sp variants, but we speculate that PITPβ-sp1 may play important roles during cytokinesis, judging by the expression of this isoform in the rapidly dividing HL60 cells. In contrast, the expression of PITPβ-sp2 in the liver, an organ whose essential function is to manufacture secretory proteins, including albumin, would suggest that PITPβ-sp2 has an important role in the secretory pathway. The importance of PITP functioning in cytokinesis is supported by studies in *Drosophila*, which contains a single Class I PITP where mutations leads to defects in cytokinesis [26,27]. *Drosophila* PITP cannot be classified as an orthologue of PITPα or PITPβ, however (see the Supplementary Figure S1 at http://www.BiochemJ.org/bj/398/bj3980411add.htm).

To understand the function of the sp variants, an essential requirement will be to have Abs that can discriminate between the PITPβ variants. As an example, in a recent analysis of PITPβ protein expression by Western-blot analysis, it was reported that the highest levels of PITPβ levels was found in brain, liver and kidney at 1.8, 1.6 and 1.2 ng/100 μg of tissue protein, whereas no PITPβ was found in heart, intestine or stomach [28]. The results presented here show much higher levels of expression in liver compared with brain (see Figure 3B) and, secondly, we readily detect PITPβ in heart and stomach. We would suggest that these results are very likely an underestimate, as the Abs used in that study might not recognize the sp variant of PITPβ. Therefore, until specific Abs for the two sp variants are available, it is essential that the published literature which has used Abs to PITPβ is interpreted with caution and that one takes into consideration the presence of the sp variants. Alternative splicing generates complexity in multicellular eukaryotes by increasing protein diversity, and estimates indicate that between 35 and 60 % of human genes yield protein isoforms by means of alternatively spliced mRNA [29]. A recent analysis of differentially spliced genes indicate that, in many instances, the alternatively spliced fragments are disordered regions [30] which are commonly responsible for protein function [30–32]. The C-terminus of PITPs is disordered [6–8,23], suggesting that this region is a major determinant of specificity in the targeting of PITPs to different cellular compartments.

Work in S. C.'s laboratory is funded by the Welcome Trust.

REFERENCES

1 Wirtz, K. W. A. (1997) Phospholipid transfer proteins revisited. Biochem. J. **324**, 353–360

2 Hsuan, J. and Cockcroft, S. (2001) The PITP family of phosphatidylinositol transfer proteins. Genome Biol. **2**, 3011.1–3011.8

3 Hamilton, B. A., Smith, D. J., Mueller, K. L., Kerrebrock, A. W., Bronson, R. T., Berkel, V. v., Daly, M. J., Kroglyak, L., Reeve, M. P., Nernhauser, J. L. et al. (1997) The *vibrator* mutation causes neurogeneration via reduced expression of PITPα: positional complementation cloning and extragenic suppression. Neuron **18**, 711–722

4 Alb, Jr, J. G., Cortese, J. D., Phillips, S. E., Albin, R. L., Nagy, T. R., Hamilton, B. A. and Bankaitis, V. A. (2003) Mice lacking phosphatidylinositol transfer protein α exhibit spinocerebellar degeneration, intestinal and hepatic steatosis, and hypoglycemia. J. Biol. Chem. **278**, 33501–33518

5 Alb, Jr, J. G., Phillips, S. E., Rostand, K., Cui, X., Pinxteren, J., Cotlin, L., Manning, T. G. S., York, J. D., Sontheimer, J. F., Collawn, J. F. and Bankaitis, V. A. (2002) Genetic ablation of phosphatidylinositol transfer protein function in murine embryonic stem cells. Mol. Biol. Cell **13**, 739–754

6 Vordtriede, P. B., Doan, C. N., Tremblay, J. M., Helmkamp, Jr, G. M. and Yoder, M. D. (2005) Structure of PITPβ in complex with phosphatidylcholine: comparision of structure and lipid transfer to other PITP isoforms. Biochemistry **44**, 14760–14771

7 Yoder, M. D., Thomas, L. M., Tremblay, J. M., Oliver, R. L., Yarbrough, L. R. and Helmkamp, Jr, G. M. (2001) Structure of a multifunctional protein. Mammalian phosphatidylinositol transfer protein complexed with phosphatidylcholine. J. Biol. Chem. **276**, 9246–9252

8 Tilley, S. J., Skippen, A., Murray-Rust, J., Swigart, P., Stewart, A., Morgan, C. P., Cockcroft, S. and McDonald, N. Q. (2004) Structure–function analysis of human phosphatidylinositol transfer protein α bound to phosphatidylinositol. Structure **12**, 317–326

9 De Vries, K. J., Westerman, J., Bastiaens, P. I. H., Jovin, T. M., Wirtz, K. W. A. and Snoek, G. T. (1996) Fluorescently labeled phosphatidylinositol transfer protein isoforms (α and β) microinjected into fetal bovine heart endothelial cells, are targeted to distinct intracellular sites. Exp.Cell Res. **227**, 33–39

10 Larijani, B., Allen-Baume, V., Morgan, C. P., Li, M. and Cockcroft, S. (2003) EGF regulation of PITP dynamics is blocked by inhibitors of phospholipase C and of the Ras–MAP kinase pathway. Curr. Biol. **13**, 78–84

11 Snoek, G. T., van Tiel, C. M. and Egmond, M. R. (2004) Structure–function relationships of phosphatidylinositol transfer proteins: involvement of phosphorylation sites. Biochimie **86**, 857–864

12 van Tiel, C. M., Westerman, J., Paasman, M. A., Hoebens, M. M., Wirtz, K. W. and Snoek, G. T. (2002) The Golgi localization of phosphatidylinositol transfer protein β requires the protein kinase C-dependent phosphorylation of serine 262 and is essential for maintaining plasma membrane sphingomyelin levels. J. Biol. Chem. **277**, 22447–22452

13 Morgan, C. P., Skippen, A., Segui, B., Ball, A., Allen-Baume, V., Larijani, B., Murray-Rust, J., McDonald, N., Sapkota, G., Morrice, N. A. and Cockcroft, S. (2004) Phosphorylation of a distinct structural form of phosphatidylinositol transfer protein α at Ser^{166} by protein kinase C disrupts receptor-mediated phospholipase C signalling by inhibiting delivery of phosphatidylinositol to membranes. J. Biol. Chem. **279**, 47159–47171

14 Skippen, A., Jones, D. H., Morgan, C. P., Li, M. and Cockcroft, S. (2002) Mechanism of ADP-ribosylation factor-stimulated phosphatidylinositol 4,5-bisphosphate synthesis in HL60 cells. J. Biol. Chem. **277**, 5823–5831

15 Segui, B., Allen-Baume, V. and Cockcroft, S. (2002) Phosphatidylinositol transfer protein-β displays minimal sphingomyelin transfer activity and is not required for biosynthesis and traffficking of sphingomyelin. Biochem. J. **366**, 23–34

16 Swigart, P., Insall, R. H., Wilkins, A. and Cockcroft, S. (2000) Purification and cloning of phosphatidylinositol transfer proteins from *Dictyostelium discoideum*: Homologues of both mammalian PITPs and *S. cerevisiae* Sec14p are found in the same cell. Biochem. J. **347**, 837–843

17 Allen-Baume, V., Segui, B. and Cockcroft, S. (2002) Current thoughts on the phosphatidylinositol transfer protein family. FEBS Lett. **531**, 74–80

18 Strausberg, R. L., Feingold, E. A., Grouse, L. H., Derge, J. G., Klausner, R. D., Collins, F. S., Wagner, L., Shenmen, C. M., Schuler, G. D., Altschul, S. F. et al. (2002) Generation and initial analysis of more than 15,000 full-length human and mouse cDNA sequences. Proc. Natl. Acad. Sci. U.S.A. **99**, 16899–16903

19 Page, M. J., Amess, B., Townsend, R. R., Parekh, R., Herath, A., Brusten, L., Zvelebil, M. J., Stein, R. C., Waterfield, M. D., Davies, S. C. and O'Hare, M. J. (1999) Proteomic definition of normal human luminal and myoepithelial breast cells purified from reduction mammoplasties. Proc. Natl. Acad. Sci. U.S.A. **96**, 12589–12594
20 Garfin, D. E. and Deutscher, M. P. (1990) Methods Enzymol. **182**, 459–477
21 Westerman, J., De Vries, K. J., Somerharju, P., Timmermans-Herejgers, J. L., Snoek, G. T. and Wirtz, K. W. (1995) A sphingomyelin-transferring protein from chicken liver. Use of pyrene-labeled phospholipid. J. Biol. Chem. **270**, 14263–14266
22 De Vries, K. J., Heinrichs, A. A. J., Cunningham, E., Brunink, F., Westerman, J., Somerharju, P. J., Cockcroft, S., Wirtz, K. W. A. and Snoek, G. T. (1995) An isoform of the phosphatidylinositol transfer protein transfers sphingomyelin and is associated with the Golgi system. Biochem. J. **310**, 643–649
23 Schouten, A., Agianian, B., Westerman, J., Kroon, J., Wirtz, K. W. and Gros, P. (2002) Structure of apo-phosphatidylinositol transfer protein α provides insight into membrane association. EMBO J. **21**, 2117–2121
24 Xie, Y., Ding, Y.-Q., Hong, Y., Feng, Z., Navarre, S., Xi, C.-X., Wang, C.-L., Zhu, X.-J., Ackerman, S. L., Kozlowski, D. et al. (2005) Role of phosphatidylinositol transfer protein α in netrin-1-induced PLC signalling and neurite outgrowth. Nat. Cell Biol. **7**, 1124–1132
25 Cunningham, E., Tan, S. W., Swigart, P., Hsuan, J., Bankaitis, V. and Cockcroft, S. (1996) The yeast and mammalian isoforms of phosphatidylinositol transfer protein can all restore phospholipase C-mediated inositol lipid signalling in cytosol-depleted RBL-2H3 and HL60 cells. Proc. Natl. Acad. Sci. U.S.A. **93**, 6589–6593
26 Giansanti, M. G., Bonaccorsi, S., Kurek, R., Farkas, R. M., Dimitri, P., Fuller, M. T. and Gatti, P. (2006) The Class I PITP Giotto is required for *Drosophila* cytokinesis. Curr. Biol. **16**, 195–201
27 Gatt, M. K. and Glover, D. M. (2006) The *Drosophila* phosphatidylinositol transfer protein encoded by *vibrator* is essential to maintain cleavage-furrow ingression in cytokinesis. J. Cell Sci. **119**, 2225–2235
28 van Tiel, C. M., Schenning, M., Snoek, G. T. and Wirtz, K. W. (2004) Overexpression of phosphatidylinositol transfer protein beta in NIH3T3 cells has a stimulatory effect on sphingomyelin synthesis and apoptosis. Biochim. Biophys. Acta **1636**, 151–158
29 Stamm, S., Ben Ari, S., Rafalska, I., Tang, Y., Zhang, Z., Toiber, D., Thanaraj, T. A. and Soreq, H. (2005) Function of alternative splicing. Gene **344**, 1–20
30 Romero, P. R., Zaidi, S., Fang, Y. Y., Uversky, V. N., Radivojac, P., Oldfield, C. J., Cortese, M. S., Sickmeier, M., Legall, T., Obradovic, Z. and Dunker, A. K. (2006) Alternative splicing in concert with protein intrinsic disorder enables increased functional diversity in multicellular organisms. Proc. Natl. Acad. Sci. U.S.A. **103**, 8390–8395
31 Dunker, A. K., Cortese, M. S., Romero, P., Iakoucheva, L. M. and Uversky, V. N. (2005) Flexible nets. The roles of intrinsic disorder in protein interaction networks. FEBS J. **272**, 5129–5148
32 Uversky, V. N., Oldfield, C. J. and Dunker, A. K. (2005) Showing your ID: intrinsic disorder as an ID for recognition, regulation and cell signaling. J. Mol. Recognit. **18**, 343–384

Received 20 March 2006/5 June 2006; accepted 13 June 2006
Published as BJ Immediate Publication 13 June 2006, doi:10.1042/BJ20060420